Multifractality in postural sway supports quiet eye training in aiming tasks: A study of golf putting

Noah Jacobson[1], Quinn Berleman-Paul[1], Madhur Mangalam[2] and Damian G. Kelty-Stephen[1]

[1]Department of Psychology, Grinnell College, Grinnell, IA 50112, USA

[2]Department of Physical Therapy, Movement and Rehabilitation Sciences, Northeastern University, Boston, MA 02115, USA

Author for correspondence:

Damian G. Kelty-Stephen

e-mail: keltysda@grinnell.edu

Ethics statement. All participants provided verbal and written informed consent approved by the Institutional Review Board (IRB) at Grinnell College (Grinnell, IA).

Data accessibility. All data analyzed in the present study are available upon request.

Author contributions: N.J., Q.B-P., and D.G.K-S. conceived and designed research; N.J., Q.B-P., and D.G.K-S. performed experiments; N.J., Q.B-P., and D.G.K-S. analyzed data; N.J., Q.B-P., M.M., and D.G.K-S. interpreted results of experiments; M.M. and D.G.K-S. prepared figures; N.J. and D.G.K-S. drafted manuscript; N.J., Q.B-P., M.M., and D.G.K-S. edited and revised manuscript; N.J., Q.B-P., M.M., and D.G.K-S. approved final version of manuscript.

Competing interests. The authors have no competing interests to declare.

Supplementary materials

Supplementary Table S1. Subset of Poisson regression model output including main and interaction effects of time and perturbation of eye height.

Abstract

The 'quiet eye' (QE) approach to visually-guided aiming behavior invests fully in perceptual information's potential to organize coordinated action. Sports psychologists refer to QE as the stillness of the eyes during aiming tasks and increasingly into self- and externally-paced tasks. Amidst the 'noisy' fluctuations of the athlete's body, quiet eyes might leave fewer saccadic interruptions to the coupling between postural sway and optic flow. Multifractality in postural sway is a robust predictor of both visual and haptic perceptual responses. Postural sway generates optic flow centered on an individual's eye height. So, we manipulated the eye height part way through a golf-putting task for participants trained in QE or trained technically as per conventional golf putting. We predicted that perturbing the eye height by attaching wooden blocks below the feet would perturb the putting more so in QE-trained participants than in those trained technically. We also predicted that responses to this perturbation would depend on multifractality in postural sway. Specifically, we predicted that less multifractality would predict more adaptive responses to the perturbation and higher putting accuracy. Results supported both predictions. QE training and lower multifractality led to more frequent successful putts, and the perturbation of eye height led to less frequent successful putts, particularly for QE-trained participants. Models of radial error (i.e., the distance between the ball's final position and the hole) indicated that lower estimates of multifractality due to nonlinearity coincided with a more adaptive response to the perturbation. These results challenge the past suggestions that reduced multifractality might be a signature of diseased posture. Instead, they suggest that reduced multifractality may act in a context-sensitive manner to restrain motoric degrees of freedom to achieve the task goal.

Keywords: biotensegrity, degree of freedom, fractal, posture, tensegrity, visual adaptation

1. Introduction

Aiming our behaviors into the visible world requires an ongoing awareness of how our body fits in the world around it. The difficulty of sorting out this bodily fit finds its classic encoding in the 'degrees of freedom' problem: an explicit choreography of goal-directed movement that stipulates all individual motoric degrees of freedom at fine `grains proves daunting and probably too rigid to be adapted to change in task or context [1]. However, another perspective suggests that the abundance of degrees of freedom is not a problem but a 'blessing' [2]. According to this view, there is no infinitude of motoric variables to stipulate at very fine grains, and on the contrary, task or intention organizes the movement system at the relatively coarse grain of the whole body and context [3]. This positive view of motor abundance appears in recent studies of aiming behaviors like the golf swing, whereby a clearly defined target in the context draws visual attention away from specific postures of the body, and indeed, experts with their eyes on the target show no single optimized mode of execution [4]. Hence, instead of requiring explicit choreography, the movement system's organization may readily emerge from perceptual linkages to the surrounding context [5–7].

1.1. Quiet eye versus technical training

Supporting task performance by emphasizing perceptual linkages versus explicit choreography is a clear theme of research on 'quiet eye' (QE). Sports psychologists refer to QE as the stillness of the eyes during aiming tasks, specifically the final gaze fixation 100 ms in duration within 3 degrees of visual angle immediately before the movement is initiated [8]. In the case of a golf swing, 'technical training' that communicates an explicit choreography of the arm and leg placement leads to less accuracy than a 'quiet eye' (QE) strategy. Experts show more frequent and longer gaze fixations on specific aspects of the putting situation (e.g., golf ball, putting surface, target hole). Novices tend to fixate more introvertedly (e.g., on the clubhead during the backswing phase) and focus on the ball only after it has been hit with the club [9–13]. Visual guidance by focusing on the target leads to a more effective golf swing than technical training of the postures and limb movements composing a golf swing. Indeed, in contrast with technical training, QE training of golf putting leads to improved putting accuracy as well as to a reduction in heart rate and muscle activity at the moment of impact [11]. Thus, it is believed that instructing athletes by directing their perceptual linkages outward to the visual field supports higher task performance as well as leads to more expert-like movement and physiology.

QE research opens a fascinating vantage point to situate ongoing research on linkages anchoring organisms to their visual contexts and the synergies transforming visual information into action (e.g., [14–16]). Research on QE has mostly examined the visual-cognitive bases for the relatively more extraverted gaze into the task context [8,17,18], and the relationship of QE to the body, the brain, and the nervous system has received relatively less attention [19–21]. To fill this gap, a 'postural-kinematic hypothesis' has begun to complement the canonical 'visual hypothesis' that QE was a primarily visual-cognitive mechanism [22]. So far, this postural-kinematic hypothesis emphasizes only slower movement times, that is, longer duration offering the foundation for longer fixations. This postural-kinematic hypothesis is a constructive first step. In this study, we aim to embed more of the postural dynamics into this hypothesis, beyond simply movement duration. Additionally, instead of reporting on gaze measurements, we will use QE as a training manipulation and focus on investigating how postural sway supports the effect of the training.

1.2. Optic flow and postural sway can support the quiet eye strategy

A crucial consideration for postural-kinematic contributions to visually guided tasks is optic flow [5–7]. Amidst the 'noisy' fluctuations of the athlete's body, quieting the eyes might leave fewer saccadic interruptions to the coupling between optic flow and postural sway. Optic flow consists of the differential expansion, contraction, or rotation of visible objects and surfaces as an individual moves

about. It is specific to both the individual's movement and the contextual layout of objects and surfaces. Indeed, virtual visual displays that impose artificial optic flow also engender anticipatory behaviors (e.g., steering, braking) as if the objects and surfaces entailed by the optic flow are out there —not just for humans but for other animal species and even robots [23]. Although most prominent in locomotion-related contexts, postural sway is no less capable of generating informative optic flow in non-locomotion contexts [24]. Because research on QE has mostly focused on the fixation of the eye gaze, QE's relationship to optic flow remains a critical gap [25].

The present work aims to replicate the beneficial effects of QE on putting performance, and more importantly, to understand how eye height and optic flow might support QE. Specifically, assuming that QE might depend on the optic flow, we aim to test whether perturbing the optic flow parameter of eye height perturbs the effect of QE training in golf putting more so than technical training. Indeed, experimentally varying eye height is known to complicate optic flow in ways that briefly perturbs visual perception (e.g., [26]). We used a single session in the style of Moore et al.'s [11] golf-putting training paradigm to test for rapid attunement to changes in information from optic flow and postural sway. For instance, manipulating eye height by adding wooden blocks to participants' shoes alters their affordance judgments significantly, leading to an initial underestimation of the optimal climbing height for a stair and sitting height for a chair. However, participants adjust to the new eye height and make more accurate decisions later on [27,28]. Hence, we expect that adding wooden blocks—(henceforth, 'clogs', to distinguish from 'blocks' of experimental trials)—to the feet might upset putting accuracy in the QE-trained participants initially, but that this accuracy will rebound as participants adjust to new eye height [8].

1.3. Multiscaled organization of postural sway entails a multifractal structure

Besides our manipulation of eye height, our expectations about the optic-flow foundation for QE also include a hypothesis about how postural sway should moderate the effects of perturbed eye height. If optic flow supports QE, we expect that QE-trained response to eye height perturbation will depend on postural sway. Indeed, in the affordance research on reattunement to perturbation of eye height, postural sway supported the adaptation of the relationship of eye height to judgments of optimal chair height for sitting [28]. However, it was not simply that more sway facilitated this adaptation because, for instance, an 'awkward stance' requiring more compensatory postural adjustments did not support visual adaptation as much as comfortable standing did. An additional challenge in identifying what portion of sway could support adaptation to altered eye height is that sway depends on events at multiple timescales. At longer scales, QE training itself might influence sway by training an explicit use of visual information. At shorter timescales, adding clogs might destabilize posture initially, and then at the shortest timescales, sway might be implicated in adapting to this perturbation of eye height. Hence, judiciously accounting the sway's contribution to visual adaptation due to perturbation of eye height requires an appreciation of sway's multi-scaled organization.

The multi-scaled organization of sway may itself reveal a key to predicting—if not explaining —how the movement system adapts its visually-guided actions. Interactions across multiple timescales noted above are currently understood to entail a 'multifractal' structure in sway. Multifractality refers to multiple (i.e., 'multi-') relationships between fluctuations and timescales, with these relationships following power laws with potentially fractional (i.e., '-fractal') exponents. Interactions across timescales engender a nonlinear patterning of fluctuations that multifractal analysis is well-poised to diagnose and quantify [29]. Specifically, multifractal analysis estimates a spectrum of fractal exponents whose width W_{MF} quantifies multifractality. When we compare measured series' W_{MF} to spectrum widths of a set of best-fitting linear models ('linear surrogates') of those series, multifractal evidence of nonlinearity manifests as a significant difference between W_{MF} for the original series and the average W_{MF} for linear surrogates. The *t*-statistic, t_{MF}, comparing the original series' W_{MF} to the surrogates' W_{MF}

serves as an estimate of how much multifractality in the original series is due to nonlinear interactions across timescales.

1.4. Multifractal nonlinearity predicts perceptual responses to perturbations of task constraints

Multifractality, W_{MF}, in postural sway is a robust predictor of perceptual responses in both visual and haptic media [30–32]. Multifractal nonlinearity, t_{MF}, in postural sway predicts perceptual responses as well, not just in the case of nonvisual judgments of length and heaviness of manually-wielded objects [33] but also in visuomotor tasks [34,35] and in response to perturbations, such as those due to prismatic goggles in a visual aiming task [36]. Now, we aim to test whether t_{MF} can predict the responses to perturbations of eye height in QE-trained golf putting.

We expected that postural sway most robust to the perturbation of eye height would show relatively narrow multifractal spectra that would still differ significantly from those of the surrogates. So far, postural sway shows relatively narrower multifractal spectra (i.e., smaller W_{MF}) for younger participants [37], those less likely to experience motion sickness [38], and those focusing on more proximal surfaces in optic flow [39]. Hence, greater W_{MF} in postural sway might counteract any effects of QE. All these findings are qualified by a failure of W_{MF} to correlate with canonical measures of sway like standard deviation. However, postural stability is only ambiguously related to the standard deviation of sway, requiring neither too much nor too little variability in sway [40,41]. Meanwhile, both empirical and theoretical work suggests that t_{MF} is more closely related to postural stabilizing. Evidence shows that postural stabilization following a perturbation to the base of support shows a rapid reduction of t_{MF} [42]. The theoretical simulation also predicts that random perturbations to individual scales of a nested system lead to multifractality due to nonlinearity and narrower multifractal spectra (i.e., smaller W_{MF} and smaller-yet-significant t_{MF}; [43]). Hence, incorporating the visual information due to the perturbation of eye height adaptively into the movement system must involve exhibiting smaller-yet-significant t_{MF}.

1.5. Golf-putting task and hypotheses

The participants were instructed to take golf putts towards a circular, hole-sized target painted on a green putting surface in the laboratory—over four blocks of ten trials each. One group received QE training, and the other group received technical training specifying how to move their limbs to make the golf putt. Wooden clogs were attached to the feet of all participants to perturb their eye height. Putting performance was treated both dichotomously (i.e., ‘making’ or ‘missing’ the putt) and continuously (i.e., in terms of radial error). We tested hypotheses specific to these two treatments.

1.5.1. Hypothesis-1: Effects on dichotomous treatment of putting performance

Putting performance was dichotomized as a ‘make’ when the golf ball came to rest within the target or 2 feet directly beyond it, and as a ‘miss’ in all other cases. We predicted that QE training would lead to more ‘makes’ (Hypothesis-1a) and that the eye height perturbation due to clogs would lead to more misses following QE training than technical training (Hypothesis-1b). We also predicted that greater sway W_{MF} would lead to fewer ‘makes’ (Hypothesis-1c).

1.5.2. Hypothesis-2: Effects on continuous treatment of putting performance

Putting performance was treated continuously in terms of unsigned radial distance from the target (i.e., unsigned radial error). We hypothesized that the eye height perturbation due to clogs would lead to lower putting accuracy characterized by higher unsigned radial error following QE training than technical training. In contrast to logistic modeling of a dichotomous dependent variable, which is limited by the number of valid predictors (e.g., [44]), a continuous dependent variable allows testing more complex hypotheses. We predicted that the above effects of clogs on QE would depend on the multifractal nonlinearity, t_{MF}, of sway beyond any effects of multifractality (i.e., W_{MF}) alone

(Hypothesis-2a). We also predicted that lower t_{MF} of sway would be associated with more flexible responses to the eye height perturbation, leading to a gradual increase but a subsequent decay of radial error across trials within the blocks with the clogs on (Hypothesis-2b).

2. Methods

2.1. Participants

Twenty undergraduate students (11 women, *mean*±1*s.d.* age = 19.5±1.2 years, all right-handed [45]) with normal or corrected vision participated in this study. All participants provided written informed consent approved by the Institutional Review Board (IRB) at Grinnell College (Grinnell, IA).

2.2. Procedure

In an hour-long session, the participants completed a single putt on each of 40 trials. Prior to the training trials, half of the participants received QE instructions (Table 1, left column) while the other half received technical putting instruction (Table 1, right column), replicating Moore et al.'s [11] methodology. The technical instructions mirrored the QE instructions but did not describe the eye-related behaviors, hence mimicking standard golf instructions. After verbally confirming that they understood the instructions, the participants watched a video demonstrating a QE-specific putting stroke (https://www.youtube.com/watch?v=lfWuL1klbsY&feature=youtu.be) or a standard putting stroke (https://www.youtube.com/watch?v=HOYZn4MYmDI). The researcher directed the quiet-eye trained participants to the key features of the golfer's gaze control and the technically-trained participants to the putting mechanics.

The participant performed the golf putts on a 6×15 feet standard indoor All Turf Matts™ artificial turf mat using a 1.68-inch diameter PING Sigma 2 Anser Stealth™ putter and regular-sized white golf balls. The participants completed straight putts ten feet away towards a 2.5-inch diameter circular orange dot, designed to fit the golf ball. This format allowed for more stringent measurement and gave the participants a more focused target.

The participants completed 20 training trials (treated as two blocks of 10 trials per block in regression modeling). Following a short 5-minute break, the participants completed two blocks of ten test trials per block (i.e., 20 test trials total) in the absence of instructions. The participants were randomly assigned to complete either their first or second block of ten trials while wearing 5-cm-raised wooden blocks (i.e., clogs) attached to their shoes (they completed the other block of ten test trials under the same conditions as the 20 training trials). Before the testing began, the participants were allowed to walk around and adjust to the clogs to reduce fall risk.

2.3. Measures

The task performance was defined in terms of the radial error (the distance from the target at which the ball stopped, in feet) and the number of putts successfully 'holed.' Because the target was not a real hole, the putt was counted as holed in either of two events: the ball came to rest within the orange dot on the floor or within 2 feet directly beyond the hole. In either of these cases, the radial error was recorded as zero [46,47]. Postural sway was measured using a smartphone with the Physics Toolbox Suite application (http://vieryasoftware.net) strapped to the participants' lower back. The app recorded the acceleration of the torso along *x*-, *y*-, and *z*-dimensions at 100 Hz. An experimenter manually started and stopped recording for each putt. Recording began after the participant set up over the ball and stopped once the ball stopped moving.

2.4. Multifractal analysis

2.4.1 Multifractal spectrum width of accelerometer displacement series

For each putt, we computed an accelerometer displacement series for multifractal analysis as follows. The accelerometer data encodes an N-length series of accelerations of the torso along *x*-, *y*-, and *z*-dimensions centered on an origin on the smartphone. A displacement series of length $N-1$ was computed by: 1) taking the first differences for the variable (e.g., if we use the letters *i* and *j* to indicate individual values in sequence, $x_{diff}(j)=x(i)-x(i-1)$ for each *i*th value of *x*, for $2<i<N$, $1<j=i-1<N-1$, 2) squaring and summing the differences of each dimension's displacements (i.e., $x_{diff}^2+y_{diff}^2+z_{diff}^2$), and 3) taking the square root of this sum (i.e., $\sqrt{(x_{diff}^2+y_{diff}^2+z_{diff}^2)}$).

Multifractal spectra $f(\alpha)$ were estimated for each accelerometer displacement series, using Chhabra and Jensen's [48] method. The first step was to partition the series into subsets (or 'bins') of various sizes, from four points to a fourth of series' length (figure 1, left). The second step was to examine how the proportion of displacements within each bin changed with bin size or timescale (figure 1, right). The third step was to estimate two distinct exponents: an exponent α describing how the average proportion grows with bin size and an exponent f describing how Shannon's [49] entropy of bin proportion changes with bin size. The later steps were all iterations of this third step, calculating a mass μ by applying an exponent q to bin proportions and using $\mu(q)$ to weight proportions selectively according to proportion size. q greater than 1 weights larger-proportion bins, and q lesser than 1 weights smaller-proportion bins (figure 2, left). q-based mass $\mu(q)$-weighting generalizes single α and f estimates from earlier steps into continual $\alpha(q)$ and $f(q)$—with $\alpha(q)$ describing how mass-weighted average bin proportion changes with bin size and $f(q)$ describing how Shannon's entropy of bin masses $\mu(q)$ with bin size (figure 2, top right).

Multifractal analysis quantifies heterogeneity as variety in $\alpha(q)$ and $f(q)$. The ordered pairs ($\alpha(q)$, $f(q)$) constitutes the multifractal spectrum (figure 2, bottom right). We included $\alpha(q)$ and $f(q)$ only when mass-weighted proportions were defined and when both of their corresponding relationships to bin size correlated at $r > 0.995$ on logarithmic plots, for bin sizes $4, 8, 12, \ldots N/4$ and $-300<q<300$, where N is the number of samples in the series.

2.4.2. Surrogate comparison

Multifractal spectrum width is sensitive to nonlinear interactions across timescales as well as to linear temporal structure. Hence, evidence of nonlinear interactions across timescales requires comparing the original series' multifractal spectrum width W_{MF} to those computed for a sample of linear surrogate series (figure 3). These linear surrogate series retain the same value as the original series but in a different order that preserves the original series' linear autocorrelation but destroys original sequence (i.e., iterative amplitude-adjusted Fourier-transform or IAAFT [29,50]; figures 4*a* to *d*). Comparing W_{MF} of the original and surrogate series (figures 4*e*, *f*) produces a *t*-statistic t_{MF}, a measure of nonlinear interactions across timescales that is standardized across series with differing linear temporal structure. t_{MF} was computed for each original series.

2.5. Mixed-effects modeling

The data were submitted to two kinds of mixed-effect modeling, namely, logistic and Poisson, using the 'glmer' function in R package *lme4* [51]. The subsequent subsections provide details of the predictors and the models.

2.5.1. Effects of time

The effects of time were modeled using trial number within a block ($trial_{block}$), block number (block), and interactions of trial number with block number ($trial_{block}$ × block), and trial number across blocks ($trial_{exp}$). The model used orthogonal polynomials of each of both predictors up to 3rd order (i.e., cubic).

The primary reason for the polynomial terms was to reveal how and when the perturbation of wearing clogs might manifest and consequently subside. Cubic polynomials allow the simplest way to accomplish this goal by allowing a peak and a flat, quiescent portion as part of the same continuous function. Additionally, unlike the quadratic function, the cubic peak is not required to be symmetric and occurring at the midpoint. Hence, the cubic function controls for any nonlinearities in the normal course of trials without such perturbations. Whereas block is a linear effect across blocks, including $\text{trial}_{\text{exp}}$ in the model allowed controlling for nonlinear change across blocks.

There are two important features to note about the treatment of time in this model. First, the Poisson model encoded both classifications of trial numbers (i.e., $\text{trial}_{\text{exp}}$ and $\text{trial}_{\text{block}}$) in terms of an orthogonal 3rd-order polynomial, using the function 'poly' in *R*, to include the linear, quadratic and cubic growth of trial number with all three terms phase-shifted so as to be uncorrelated with one another. Second, the lack of model convergence limited the appearance of block, such that block was neither treated nonlinearly nor in interaction with perturbation. Attempting to include the orthogonal 3rd-order polynomials for block number led to a failure of model convergence, so block only appeared as a linear term. The model also failed to converge when it included interactions of block and perturbation because these two terms were strongly collinear.

2.5.2. Effects of manipulations

Manipulations included quiet-eye instruction, QE (QE = 1 for receiving QE instruction, and QE = 0 for not receiving QE instruction) and perturbation of eye height, perturbation (perturbation = 1 for all ten trials during the block when participants wore the clogs, and perturbation = 0 for all other trials).

2.5.3. Sway: Linear predictors

The accelerometer data encodes accelerations of the torso along *x*-, *y*-, and *z*-dimensions. Any single posture corresponds to a specific point in this 3D space. Hence, sway corresponds to the deviation of this 3D acceleration around the mean posture. The present analyses encoded this variability as MSD_{acc} or $RMS_{\text{acc,}}$ depending on which predictor supported a convergent model, along with mean and standard deviation of 3D displacement ($Mean_{\text{disp}}$ and SD_{disp}, respectively).

2.5.4. Models

A mixed-effects logistic regression modeled the odds of a successful putt (i.e., a 'make,' vs. a 'miss'), which included all putts ending with the golf ball coming to rest within the orange dot on the floor or within 2 feet directly beyond the hole. Predictors included QE × perturbation (as well as lower-order component main effects QE and perturbation; e.g., [52]) to test Hypotheses-1a and -1b, and W_{MF} to test Hypothesis-1c, as well as block and RMS_{acc} to control for the effects of practice and linear structure of postural sway. Additional predictors did not significantly improve model fit and hence were omitted. A mixed-effects linear regression modeled the radial error (in inches) of all misses, with makes as defined above treated as having a zero radial error. Predictors for this second model included QE × perturbation × $\text{trial}_{\text{block}}$ × t_{MF} to test Hypothesis-2 by specifically addressing trials within each block, QE × $\text{trial}_{\text{block}}$ and QE × $\text{trial}_{\text{exp}}$ to control for differences in learning due to QE across a linear progression of block; a nonlinear function of trials, QE × perturbation × W_{MF} × t_{MF}, to control for the effects of multifractal spectral width and its relationship with t_{MF}; and MSD_{acc} × $Mean_{\text{disp}}$ × SD_{disp} to control for the effects of linear description of sway.

3. Results

3.1. Testing hypothesis-1: Odds of a make increased with QE, decreased with the perturbation of eye height, with a more negative effect of the perturbation for the QE group

A mixed-effect logistic regression model of successful putting (i.e., the 'makes') returned the coefficients reported in Table 2. Predictors for t_{MF} and for interactions of QE with all terms other than perturbation failed to improve model fit significantly and so were omitted from the final model. This model failed to return an effect of QE ($b = 0.20$, *s.e.m.* = 0.30, $p = 0.51$), failing to support Hypothesis-1a. The perturbation failed to show a significant effect of the perturbation alone ($b = –0.22$, *s.e.m.* = 0.43, $p = 0.60$). However, there was a moderately significant negative effect of QE × perturbation ($b = –1.16$, *s.e.m.* = 0.65, $p = 0.07$), suggesting that the participants instructed to use the QE strategy had marginally worse odds of a successful putt in the face of the perturbation, that is, 0.30 of the odds of non-QE participants in the face of the perturbation. This result gave only marginal support to Hypothesis-1b.

There were also effects of experience and trial-by-trial sway. Block had a positive effect ($b = 0.24$, *s.e.m.* = 0.13, $p = 0.06$), suggesting that odds of a successful putt was 1.27 times higher with each successive block of trials. RMS_{acc} showed a positive effect ($b = 4.05$, *s.e.m.* = 1.34, $p < 0.0001$), and total multifractality W_{MF} showed a negative effect ($b = –7.25$, *s.e.m.* = 2.94, $p < 0.0001$), suggesting that successful putts were more likely with more variable and less multifractal accelerations of sway. This latter result supported Hypothesis-1c.

3.2. Poisson modeling of radial error

A Poisson model of trial-by-trial radial error (i.e., the Euclidean distance of the ball's final resting position from the hole's center [in feet]) returned the coefficients in Supplementary Table S1. Supplementary Table S1 describes the coefficients for the effects of time, perturbation of eye height, and of interactions between the two. Table 3 describes the coefficients for trial-by-trial accelerations in postural sway, including linear descriptors ($MSD_{acc} \times Mean_{disp} \times SD_{disp}$) and nonlinear descriptors ($MSD_{acc} \times Mean_{disp} \times SD_{disp}$, and QE × perturbation × $trial_{block} \times t_{MF}$). The full model generated predictions that correlated with the observed trial-by-trial radial error, $r = 0.54$. Figure 5 plots the observed trial-by-trial radial error and trial-by-trial model predictions on the same axis for four participants each from the technical and QE-trained groups, respectively. We detail the effects of time and perturbation in the following sections. For brevity, we will only refer to significant coefficients in text.

3.2.1. Non multifractal effects on radial error

This section details the non-multifractal effects described in Supplementary Table S1 and effects preliminary to the test of Hypothesis-2 in Table 3. Radial error grew linearly and quadratically across trials but showed negative cubic variation with trial—both for trials across the experiment and within a block (figure 5*a*). The QE strategy prompted steady decay of error across the experiment, canceling out the linear and cubic pattern of error over trials within a block (figure 5*b*). The perturbation of eye height elicited no main effect but increased the growth of error over trials within a block, with the QE instruction accentuating this nonlinear growth of error later in the block. The higher-order interaction $MSD_{acc} \times Mean_{disp} \times SD_{disp}$ and its main component effects and lower-order interactions showed mostly negative effects (only two of the two-way interactions showed positive coefficients), consonant with the positive effect for RMS_{acc} predicting greater accuracy in the logistic model (Section 3.1.).

3.2.2. Total multifractality of sway, W_{MF}, increased radial error, but multifractality due to nonlinearity, t_{MF}, attenuated radial error at the beginning and the end of blocks

Before considering what portion of multifractality is attributable to linear or nonlinear structure, the total width W_{MF} of original series' multifractal spectra is associated with greater radial error ($b = 1.80\times10^{0}$, *s.e.m.* = 1.29×10^{-1}, $p < 0.0001$). This result is incidentally supportive of Hypothesis-1c, resembling the negative effect on W_{MF} on the likelihood of a successful putt (Section 3.2.1.). We did not find any main effect of multifractality due to nonlinearity, t_{MF}, nor any interaction of $W_{MF} \times t_{MF}$.

However, the negative effect for t_{MF} × $trial_{block}$ (Quadratic; $b = -8.93\times10^{-2}$, *s.e.m.* = 1.15×10^{-2}, $p < 0.0001$) indicated an association between multifractality due to nonlinearity with a significant reduction of the positive quadratic profile for radial error over trials within a block (i.e., $trial_{block}$(Quadratic); Section 3.2.1.).

3.2.3. Testing Hypothesis-2a: Perturbation of eye height increased radial error only in combination with QE training, with greater multifractality due to nonlinearity t_{MF}, or with both

Much like the effect of trials within a block (Section 3.2.3.), the multifractality of sway promoted the tendency of QE to increase perturbation-related radial error. An important point to recall at this point is that, unlike in the logistic regression (Section 3.1.), neither did we find a main effect of perturbation not an interaction effect of QE × perturbation. Perturbation showed a significant effect through its interactions with other factors, the earliest being its interaction with $trial_{block}$ (Section 3.2.3.); the interaction of perturbation × W_{MF} ($b = -1.50\times10^{0}$, *s.e.m.* = 3.12×10^{-1}, $p < 0.0001$) canceled out the positive effect of W_{MF} on error (Section 3.2.2), suggesting that the perturbation reduced the error-eliciting effect of W_{MF}. The interaction QE × W_{MF} reduced error by roughly half ($b = -1.04\times10^{0}$, *s.e.m.* = 2.03×10^{-1}, $p < 0.0001$), suggesting that QE promoted greater accuracy but only in the absence of perturbation. However, the interaction with multifractality indicates that QE increased the error attributable to the perturbation. For instance, the QE × perturbation × W_{MF} ($b = 2.12\times10^{0}$, *s.e.m.* = 4.91×10^{-1}, $p < 0.0001$) reverses the apparently beneficial error-reducing interaction effect of perturbation × W_{MF}. Hence, QE reinstated the error due to total multifractality (Section 3.2.2), and it did so only in the face of the perturbation.

Above and beyond the effects of W_{MF} in moderating the interaction effect of QE × perturbation, t_{MF} promoted the error-increasing effect of perturbation. Specifically, besides the moderating effect of QE on the effect of perturbation × W_{MF}, perturbation elicited even greater radial error with increases in t_{MF} (perturbation × W_{MF} × t_{MF}: $b = 1.54\times10^{-1}$, *s.e.m.* = 3.15×10^{-2}, $p < 0.0001$). QE did reverse this effect (QE × perturbation × W_{MF} × t_{MF}: $b = -2.21\times10^{-1}$, *s.e.m.* = 4.97×10^{-2}, $p < 0.0001$). However, QE also increased error in combination with perturbation and t_{MF} even in the absence of any moderating effect of W_{MF} (QE × perturbation × t_{MF}: $b = 8.62\times10^{-3}$, *s.e.m.* = 4.18×10^{-3}, $p < 0.05$). This result supports Hypothesis-2a.

3.2.4. Testing Hypothesis-2b: the QE group with greater multifractal nonlinearity in sway showed a greater initial but progressively slower increase in radial error due to the perturbation of eye height

The interactions of QE × $trial_{block}$ with multifractal nonlinearity followed a similar but weaker pattern as the interactions of QE × $trial_{block}$ with perturbation. Much like the perturbation of eye height, the interaction of QE with t_{MF} accentuated the radial error late in a block of ten trials (QE × $trial_{block}$ × t_{MF}): it weakened the linear term ($b = -3.73\times10^{-2}$, *s.e.m.* = 1.46×10^{-2}, $p < 0.05$), contributing to a negative-quadratic peak in the middle of the block ($b = -1.85\times10^{-1}$, *s.e.m.* = 1.66×10^{-2}, $p < 0.0001$) and a positive cubic increase at the end of the block ($b = 1.13\times10^{-1}$, *s.e.m.* = 1.73×10^{-2}, $p < 0.0001$). Hence, t_{MF} and perturbation showed independent effects on the progression of error across trials in block.

However, the similarity of these effects independently on error across trials within a block did not extend to their interaction. Indeed, most relevant to testing Hypothesis-2b is that the interaction of perturbation and t_{MF} served to speed up the growth of error, and QE slowed it down across the block. Coefficients for perturbation × $trial_{block}$ × t_{MF} indicated that in the face of perturbation, multifractal nonlinearity removed the observed peak in error due to earlier negative quadratic effects ($b = 3.83\times10^{-1}$, *s.e.m.* = 5.28×10^{-2}, $p < 0.0001$) and increased error across the linear ($b = 4.07\times10^{-1}$, *s.e.m.* = 5.20×10^{-2}, $p < 0.0001$)and cubic terms ($b = 5.39\times10^{-1}$, *s.e.m.* = 4.45×10^{-2}, $p < 0.0001$). On the other hand, coefficients for perturbation × $trial_{block}$ × t_{MF} indicated that, in the face of perturbation for the QE

participants, the linear increase was shallower ($b = -2.71\times10^{-1}$, *s.e.m.* $= 6.11\times10^{-2}$, $p < 0.0001$), the positive quadratic growth further removed the observed peak in error ($b = 4.24\times10^{-1}$, *s.e.m.* $= 6.14\times10^{-2}$, $p < 0.0001$), and the cubic term was negative ($b = -7.90\times10^{-1}$, *s.e.m.* $= 5.79\times10^{-2}$, $p < 0.0001$).

The outcome of these differences distinguishes how multifractal nonlinearity predicted changes in adaptive responses to the perturbation of eye height. Greater t_{MF} exhibited less adaptive response to the perturbation in the QE case, and less-but-still-nonzero t_{MF} predicted a more gradual appearance of error and then a subsequent decay of this error. Greater t_{MF} led the QE group to exhibit initially greater error and a smaller change in error across trials, and lower levels of t_{MF} led the QE group to show a delayed growth in error and subsequent decay in error (figure 5*b*), suggesting adaptation. It is evident in figure 5*b* that although the error in the high-t_{MF} cases with the perturbation was smaller than the delayed increase in the low-t_{MF} cases with the perturbation, the high-t_{MF} cases showed more sustained error and no adaptation to the perturbation relative to high-t_{MF} cases without the perturbation. This result supports Hypothesis-2b.

4. Discussion

We tested two hypotheses about the role of QE training in golf putting. Our first hypothesis was that, for the dichotomous outcome of putting performance ('make' versus 'miss'), QE training would improve the odds of a make, clogs (i.e., wooden blocks added to the feet) would reduce the odds of a make in general and even more for QE trained participants, and multifractal spectrum width of sway, W_{MF}, would reduce the odds of a make as well. Our second hypothesis was that, for the continuous outcome of putting performance (radial error), the response of QE-trained participants to a perturbation of eye height would depend on the multifractality attributable to nonlinear interactions across scales, t_{MF}. We predicted that lower estimates of t_{MF} would coincide with a more adaptive response, that is, with slower growth of radial error and then with subsequent decay of radial error over trials. Results supported the first hypothesis only partially: we found no main effect of QE training, only a marginally significant disadvantage due to QE with the clogs, and a significant main effect associating greater multifractality W_{MF} with greater error. On the other hand, results strongly supported the second hypothesis that accuracy with QE depends on the multifractal nonlinearity in postural sway. In fact, the model testing second hypothesis in the Poisson model replicated the null effects for QE and its interaction with clogs from the logistic regression. This second model not only replicated the multifractal effect from the logistic model, but it also elaborated on a strong relationship of QE-trained performance with mulitifractal aspects of sway.

These results offer two major insights for research into perception-action in visual aiming tasks. First, it shows that QE training has clear roots in postural sway, vindicating and elaborating earlier proposals that quiet eye is not simply about stabilizing the eyes [53,54]. Indeed, it has long been known that simply stabilizing the retinal position compromises the persistence of a visual image [55–57]. And contrary to a colloquial understanding of 'quiet eye,' more recent work confirms that those small movements within gaze fixations called 'microsaccades' might prevent fading [58] and support visual attentional processes [59]. We might draw a comparison between the 'quiet' suggested by 'quiet eye' and that indicated by 'quiet standing.' Both 'quietudes' provide the needed instruction to a participant or athlete to 'please move as little as possible,' but below the polite clarity for verbal instruction, both 'quietudes' depend upon a rich texture of fluctuations. Fluctuations throughout the body support exploration during quiet standing [60], and quiet eye is no less an exception than quiet standing has been [5–7]. The value of QE is not necessarily a net reduction of fluctuations but rather a way to train athletes to orient their movements towards the optic flow generated by postural sway. Whereas the postural-kinematic hypothesis had previously only referred to longer movement duration [22], we now report that movements are not merely slower but evince a sort of nonlinearity constricting the degrees

of freedom across scales of the movement-system hierarchy. In one of the subsections below, we discuss how this orienting towards optic flow might coordinate with mechanisms invoked by the more elaborate visual hypothesis (e.g., [61,62]).

The second insight is that the multifractality in sway is an essential aspect of postural adaptations contributing to visually-guided action. It was already known that damping out postural perturbations could occasion a ratcheting down of multifractality in postural sway [42]. The present results indicate that this reduction of multifractality is associated with more accurate responses in visually-guided aiming. Note that this reduced multifractality remains different from corresponding surrogates. Hence, nonlinear interactions across scales can constrict movement variability, making reduced multifractality more adaptive [63–65]. This distinction is a departure from any shorthand presumption that 'more multifractal is better' supported by early studies of heart rate variability (HRV) [66]. Indeed, this departure reflects a growing clarity about the value of multifractal fluctuations for predicting and explaining outcomes in perception-action.

4.1. Clarifying the value of multifractal fluctuations for perceiving-acting systems

The shorthand 'more multifractal is better' presumptions from early studies on HRV [66] have always underestimated the more elaborate systematicity in the physiology of the human movement system with upright posture. Early work proposed that a 'loss of [fractal or multifractal] complexity' would occasion or coincide with aging or with pathology [67]. Indeed, early evidence showed that less healthy outcomes co-occurred with more-than-fractal levels of temporal correlation [68]. However, the task has always been known to influence multifractality in upright posture: multifractality of quiet standing can reduce with pathology [69,70], but multifractality in gait can increase with pathology [71], as well as with walking speeds faster or slower than self-selected comfortable speed [72]. Over the lifespan, the maturation of gait involves loss of multifractality, beginning with the stabilization of toddler gait into young adult gait and continuing into older age [73]—this lifelong progression actually is at odds with more recent evidence that multifractality in HRV remains stable with healthy aging [74].

Militating strongly against simple ''more multifractal is better' kind of presumptions are a variety of distinctions that are at once obvious but need recognition if we want to identify for what, after all, multifractality is good. These distinct points include, for instance, that hearts are not upright bipedal bodies, that age is not itself a pathology, and that walking is not standing. In the promise of fractal/multifractal analysis, the discourse about 'complexity,' 'dynamical stability,' and the role of fractality/multifractality in 'optimality' [75–77] can make no claims on all definitions of optimality and so has not been responsible for acknowledging that some multifractality is not optimal [78]. Indeed, studies in behavioral sciences have always justified the capacity of fractal variety to offer new insights [79,80]. Any notion of a privileged level or direction of fractal variety [81] might be best understood as a reaction to critical perspectives suggesting that the discourse in behavioral sciences should have much less or perhaps zero fractality or multifractality in [82]. Measurements may wax and wane in their multifractal structure. The only case in which we think more multifractality is always better than less is not in all of our measurements but rather in the scientific discourse on the coordination of movement systems engaged in perception-action.

4.2. The value of multifractal fluctuation is specific to task constraints

What is coming into focus is that the value of nonlinearity-driven multifractality depends on task context. More of it is adaptive when tasks invite exploration and anticipation. Less of it is adaptive when the task needs restraint for precise consistency and constraint. As an example of the former, accumulating information as a reader can require keeping an open mind to follow the discourse wherever it may lead, and more multifractality t_{MF} in the pacing of word-by-word reading supports more fluent reading if the story has a twist in its plot [34]. Similarly, more multifractality W_{MF} in circle-

tracing behaviors make for poor tracing but is associated with better performance on neurophysiological tests of flexibility with rule switching [83]. The freewheeling benefits of more multifractality can also compete alongside the precision-, repetition-promoting benefit of less multifractality. In a Fitts task, greater multifractality t_{MF} in hand and head movements predicted less stable contact with the targets, but it became a predictor of more stable contact when participants had the diffuse warning that they might be asked to close their eyes and continue the task [35]. Hence, what would have upset task performance became a resource for exploring the task space for the eventuality of a major loss of sensory information. And now, we see that a less multifractal postural system can be more stable (e.g., smaller t_{MF} in [42]; and smaller W_{MF} in [38,39]) and, as present findings indicate, more accurate in how it orients behaviors to a visually-guided aiming task.

Some of the task-specificity remains unclear, e.g., manual wielding of an object is more accurate with greater multifractality in postural sway, but hefting an object to perceive heaviness compared to a reference object is more accurate with less multifractality [33]. This difference could have to do with the qualities of length and heaviness, but the simpler interpretation could be that intending to perceive directs attention away from the center of pressure and intending to perceive heaviness directs attention inwards toward the center of pressure, lending length perceptions and heaviness perception to more and less postural instability. This issue of directing attention is again a reason we will need to consider how to link this postural-kinematic work on QE back with the visual-hypothesis work on QE.

The fact that reduced multifractality can be beneficial offers a unique distinction between possibly two related but distinct interpretations of multifractal results: one as a biomarker of pathology and the other as adaptation. Indeed, the loss of multifractality can be a biomarker for diagnosing a pathology [84]. The physiological wisdom informing this usage is that the heart has to be, in effect, poised to absorb and rebound from perturbations, avoiding fragility due to insult at any single characteristic scale (e.g., [67]). Implicit in this wisdom is that, within the healthy body, the heart's task is deeply anticipatory and exploratory, much like those task settings in which whole organisms benefit from more multifractality. However, hastily concluding that loss of multifractality is just symptomatic of postural systems with sensory deficits is premature and even casts too gloomy a connotation over reduced multifractality [70]. The present results with a perturbation of eye height indicate that reduced multifractality could be an adaptive response preserving stability and promoting task performance in the face of abrupt change in the organism's mechanical relationship with the base of support. Hence, far from being the signature of diseased posture, reductions in multifractality that maintain a significant t_{MF} suggest nonlinear interactions across scales acting context-sensitively to restrain motoric degrees of freedom so as to achieve the task goal.

Different task constraints prompt different modes of movement variability, and if multifractal depictions of the body seem to physicalize or mechanize the movement system, they do so only in the way that nonlinear-dynamical physical mechanisms might better explain context-sensitive behavior. Surely, good-faith pursuit into nonlinear-dynamical complexity should avoid any catch-all simplification (e.g., 'more is better, less is worse') and keep a keen eye on what sort of multifractality is good for what end. Nonlinear dynamics has also profited from consideration of its measures in different reference frames before: experimentally breaking apart the coincidence of relative-phase in spatial frames from relative-phase in muscular frames revealed novel, more generic structure in the Haken-Kelso-Bunz [85] law for multi-limb coordination [86]. Finally, considering the task frames for our interpretation of multifractal estimates may be equally crucial for generalizing predictions for a multifractal foundation for perception-action. Low multifractality in the heart signals a bad prognosis to the clinician, but low multifractality in posture supports good task performance in visually-guided aiming, particularly for an organism beset by malevolent experimenters uprooting their optic flow.

4.3. The value of multifractality is also specific to different tissues of the body.

Just as different tissues of the same body can differently support the same task, we expect that the multifractal structure that spans across these different tissues supports overarching integrity to the organismal-level behavior we measure in the laboratory [87]. Here, a comparison of present results with similar work using a relatively less-mechanical, visual perturbation [36], may tee up considerations for future work that could elaborate an explanation of QE by integrating the postural-kinematic hypothesis with the visual hypothesis. The present results resemble those of Carver et al. [36] who found that, without any training (i.e., neither QE nor technical), more multifractality in torso sway led to greater error in a low-difficulty Fitts task (compare W_{MF} in Tables 1 and 3) led to smaller error in the case of a visual perturbation (compare perturbation × W_{MF} in Table 3), that is, multifractality in head sway became a stabilizing, accuracy-promoting asset to task performance when the target was far out of reach. Future research could also probe the visual hypothesis for QE for multifractal foundations, and based on Carver et al.'s [36] results, we predict that QE-trained performance would improve with greater multifractality in head sway or eye movements. Monofractal analysis of eye movements has successfully predicted visual attention to text [88], and such fluctuations in quiet eye likely support an extension of the multifractal support for QE. The present results do not include gaze data, but we hope it is informative, especially in support of the postural-kinematic hypothesis, that the QE instructions enlist the nonlinear interactions across scales of the movement system without drawing the athlete's attention to the body.

Ultimately, this task- and anatomically-specific portrait of multifractal fluctuations rests on the even more generic facts that multifractal fluctuations spread across the body and that estimates of this spread predict the accuracy of the perceptual outcomes [89,90]. Hence, rather than inventorying body parts and task constraints prompting different values of multifractality, the longer view of investigating visually-guided aiming must examine the flow of multifractal fluctuations. Carver et al. [36] found that multifractality spread from hip to head, as well as from head and hip toward the throwing hand. Indeed, in all these studies, the body appears to direct multifractal fluctuations towards those body parts most clearly engaged in the focal tasks. We might expect similar results in golf putting. QE training may promote this spread by reducing intentional movements of the head and eyes that might interfere with upstream flows of multifractality. The direction of attention towards a distant target in the visual field may depend on stabilizing the postural grasp of the surface underfoot and shunting multifractal fluctuations toward the head and eyes. Indeed, executive functions directing attention to specific features of the visual field benefits from a rich substrate of multifractal fluctuations in the head [91], hand [92,93], and brain [94,95] that vary systematically with access to and mastery of the rules supporting task performance. When we consider that eye movements show multifractality [96] and that variability in the monofractal structure of eye movements can predict visual attention [88], we see early glimpses of a multifractal bridge from the postural-kinematic support to the visual support for QE.

The novelty of multifractal modeling to behavioral sciences can make this promise of a multifractal infrastructure supporting visually guided behaviors sound too ethereal and misty to be practical. But we can root this proposal in the known physiology spanning the very same bones, muscles, bones, joints, brain, and eyes whose coordination generates the winning golf putt. Specifically, the connective tissues composing the fascia operate to coordinate context-sensitive behavior across so wide a variety of scales (e.g. [97]) that multifractality is one of the few current compelling frameworks for modeling how it might support perception-action [98,99]. Examining how task constraints moderate a flow of multifractal fluctuations through the body could inform future explanations for QE training and other visual aiming tasks.

References

1. Bernstein NA. 1967 *The Co-ordination and Regulation of Movement*. Oxford, UK: Pergamon Press.
2. Latash ML. 2012 The bliss (not the problem) of motor abundance (not redundancy). *Exp. Brain Res.* **217**, 1–5. (doi:10.1007/s00221-012-3000-4)
3. Latash ML. 2020 On primitives in motor control. *Motor Control* **24**, 318–346. (doi:10.1123/mc.2019-0099)
4. Morrison A, McGrath D, Wallace ES. 2016 Motor abundance and control structure in the golf swing. *Hum. Mov. Sci.* **46**, 129–147. (doi:10.1016/j.humov.2016.01.009)
5. Stoffregen TA. 1985 Flow structure versus retinal location in the optical control of stance. *J. Exp. Psychol. Hum. Percept. Perform.* **11**, 554–565. (doi:10.1037/0096-1523.11.5.554)
6. Stoffregen TA. 1986 The role of optical velocity in the control of stance. *Percept. Psychophys.* **39**, 355–360. (doi:10.3758/BF03203004)
7. Stoffregen TA, Riccio GE. 1990 Responses to optical looming in the retinal center and periphery. *Ecol. Psychol.* **2**, 251–274. (doi:10.1207/s15326969eco0203_3)
8. Rienhoff R, Tirp J, Strauß B, Baker J, Schorer J. 2016 The 'quiet eye' and motor performance: A systematic review based on Newell's constraints-led model. *Sport. Med.* **46**, 589–603. (doi:10.1007/s40279-015-0442-4)
9. Vickers JN. 1992 Gaze control in putting. *Perception* **21**, 117–132. (doi:10.1068/p210117)
10. Vickers JN. 1996 Visual control when aiming at a far target. *J. Exp. Psychol. Hum. Percept. Perform.* **22**, 342–354. (doi:10.1037/0096-1523.22.2.342)
11. Moore LJ, Vine SJ, Cooke A, Ring C, Wilson MR. 2012 Quiet eye training expedites motor learning and aids performance under heightened anxiety: The roles of response programming and external attention. *Psychophysiology* **49**, 1005–1015. (doi:10.1111/j.1469-8986.2012.01379.x)
12. Vine SJ, Lee DH, Walters-Symons R, Wilson MR. 2017 An occlusion paradigm to assess the importance of the timing of the quiet eye fixation. *Eur. J. Sport Sci.* **17**, 85–92. (doi:10.1080/17461391.2015.1073363)
13. Vine SJ, Lee DON, Moore LEEJ, Wilson MR. 2013 Quiet eye and choking: Online control breaks down at the point of performance failure. *Med. Sci. Sport. Exerc.* **45**. (doi:10.1249/MSS.0b013e31829406c7)
14. Profeta VLS, Turvey MT. 2018 Bernstein's levels of movement construction: A contemporary perspective. *Hum. Mov. Sci.* **57**, 111–133. (doi:10.1016/j.humov.2017.11.013)

15. Kelty-Stephen DG, Lee I-C, Carver NS, Newell KM, Mangalam M. 2020 Visual effort moderates a self-correcting nonlinear postural control policy. *bioRxiv* , 209502. (doi:10.1101/2020.07.17.209502)

16. Mangalam M, Lee I-C, Newell KM, Kelty-Stephen DG. 2020 Visual effort moderates postural cascade dynamics. *bioRxiv* , 209486. (doi:10.1101/2020.07.17.209486)

17. Vickers JN. 2011 Mind over muscle: The role of gaze control, spatial cognition, and the quiet eye in motor expertise. *Cogn. Process.* **12**, 219–222. (doi:10.1007/s10339-011-0411-2)

18. Panchuk D, Vickers JN. 2006 Gaze behaviors of goaltenders under spatial–temporal constraints. *Hum. Mov. Sci.* **25**, 733–752. (doi:10.1016/j.humov.2006.07.001)

19. Shine JM, Aburn MJ, Breakspear M, Poldrack RA. 2018 The modulation of neural gain facilitates a transition between functional segregation and integration in the brain. *Elife* **7**, e31130. (doi:10.7554/eLife.31130)

20. Renshaw I, Davids K, Araújo D, Lucas A, Roberts WM, Newcombe DJ, Franks B. 2019 Evaluating weaknesses of "perceptual-cognitive training" and "brain training" methods in sport: An ecological dynamics critique. *Front. Psychol.* **9**, 2468.

21. Davids K, Araújo D. 2016 What could an ecological dynamics rationale offer Quiet Eye research? Comment on Vickers. *Curr. Issues Sport Sci.* **1**, 104. (doi:10.15203/CISS_2016.100)

22. Gallicchio G, Ring C. 2020 The quiet eye effect: A test of the visual and postural-kinematic hypotheses. *Sport. Exerc. Perform. Psychol.* **9**, 143–159. (doi:10.1037/spy0000162)

23. Serres JR, Ruffier F. 2017 Optic flow-based collision-free strategies: From insects to robots. *Arthropod Struct. Dev.* **46**, 703–717. (doi:10.1016/j.asd.2017.06.003)

24. Stoffregen TA, Yang C-M, Bardy BG. 2005 Affordance judgments and nonlocomotor body movement. *Ecol. Psychol.* **17**, 75–104. (doi:10.1207/s15326969eco1702_2)

25. de Oliveira RF. 2016 Visual perception in expert action. In *Performance Psychology: Perception, Aaction, Cognition, Emotion* (eds M Raab, B Lobinger, S Hoffman, A Pizzera, S Laborde), pp. 254–270. London, UK: Academic Press.

26. Frenz H, Bremmer F, Lappe M. 2003 Discrimination of travel distances from 'situated' optic flow. *Vision Res.* **43**, 2173–2183. (doi:10.1016/S0042-6989(03)00337-7)

27. Mark LS. 1987 Eyeheight-scaled information about affordances: A study of sitting and stair climbing. *J. Exp. Psychol. Hum. Percept. Perform.* **13**, 361–370. (doi:10.1037/0096-1523.13.3.361)

28. Mark LS, Balliett JA, Craver KD, Douglas SD, Fox T. 1990 What an actor must do in order to perceive the affordance for sitting. *Ecol. Psychol.* **2**, 325–366. (doi:10.1207/s15326969eco0204_2)

29. Ihlen EAF, Vereijken B. 2010 Interaction-dominant dynamics in human cognition: Beyond 1/*f* fluctuation. *J. Exp. Psychol. Gen.* **139**, 436–463. (doi:10.1037/a0019098)

30. Doyon JK, Hajnal A, Surber T, Clark JD, Kelty-Stephen DG. 2019 Multifractality of posture modulates multisensory perception of stand-on-ability. *PLoS One* **14**, e0212220. (doi:10.1371/journal.pone.0212220)

31. Hajnal A, Clark JD, Doyon JK, Kelty-Stephen DG. 2018 Fractality of body movements predicts perception of affordances: Evidence from stand-on-ability judgments about slopes. *J. Exp. Psychol. Hum. Percept. Perform.* **44**, 836–841. (doi:10.1037/xhp0000510)

32. Teng DW, Eddy CL, Kelty-Stephen DG. 2016 Non-visually-guided distance perception depends on matching torso fluctuations between training and test. *Attention, Perception, Psychophys.* **78**, 2320–2328. (doi:10.3758/s13414-016-1213-5)

33. Mangalam M, Kelty-Stephen DG. 2020 Multiplicative-cascade dynamics supports whole-body coordination for perception via effortful touch. *Hum. Mov. Sci.* **70**, 102595. (doi:10.1016/j.humov.2020.102595)

34. Booth CR, Brown HL, Eason EG, Wallot S, Kelty-Stephen DG. 2018 Expectations on hierarchical scales of discourse: Multifractality predicts both short- and long-range effects of violating gender expectations in text reading. *Discourse Process.* **55**, 12–30. (doi:10.1080/0163853X.2016.1197811)

35. Bell C, Carver N, Zbaracki J, Kelty-Stephen D. 2019 Nonlinear amplification of variability through interaction across scales supports greater accuracy in manual aiming: Evidence from a multifractal analysis with comparisons to linear surrogates in the Fitts task. *Front. Physiol.* **10**, 998. (doi:10.3389/fphys.2019.00998)

36. Carver NS, Bojovic D, Kelty-Stephen DG. 2017 Multifractal foundations of visually-guided aiming and adaptation to prismatic perturbation. *Hum. Mov. Sci.* **55**, 61–72. (doi:10.1016/j.humov.2017.07.005)

37. Munafo J, Curry C, Wade MG, Stoffregen TA. 2016 The distance of visual targets affects the spatial magnitude and multifractal scaling of standing body sway in younger and older adults. *Exp. Brain Res.* **234**, 2721–2730. (doi:10.1007/s00221-016-4676-7)

38. Koslucher F, Munafo J, Stoffregen TA. 2016 Postural sway in men and women during nauseogenic motion of the illuminated environment. *Exp. Brain Res.* **234**, 2709–2720. (doi:10.1007/s00221-016-4675-8)

39. Li R, Walter HJ, Stoffregen TA. 2020 The role of visual feedback about motion of the ground on postural sway. *J. Mot. Behav.* **52**, 352–359. (doi:10.1080/00222895.2019.1627281)

40. Chen L-C, Metcalfe JS, Chang T-Y, Jeka JJ, Clark JE. 2008 The development of infant upright posture: Sway less or sway differently? *Exp. Brain Res.* **186**, 293–303. (doi:10.1007/s00221-007-1236-1)

699 41. Rajachandrakumar R, Mann J, Schinkel-Ivy A, Mansfield A. 2018 Exploring the relationship
700 between stability and variability of the centre of mass and centre of pressure. *Gait Posture* **63**,
701 254–259. (doi:10.1016/j.gaitpost.2018.05.008)

702 42. Kelty-Stephen DG. 2018 Multifractal evidence of nonlinear interactions stabilizing posture for
703 phasmids in windy conditions: A reanalysis of insect postural-sway data. *PLoS One* **13**,
704 e0202367. (doi:10.1371/journal.pone.0202367)

705 43. Lee JT, Kelty-Stephen DG. 2017 Cascade-driven series with narrower multifractal spectra than
706 their surrogates: Standard deviation of multipliers changes interactions across scales. *Complexity*
707 **2017**, 7015243. (doi:10.1155/2017/7015243)

708 44. van Smeden M, de Groot JAH, Moons KGM, Collins GS, Altman DG, Eijkemans MJC, Reitsma
709 JB. 2016 No rationale for 1 variable per 10 events criterion for binary logistic regression
710 analysis. *BMC Med. Res. Methodol.* **16**, 163. (doi:10.1186/s12874-016-0267-3)

711 45. Oldfield RC. 1971 The assessment and analysis of handedness: The Edinburgh inventory.
712 *Neuropsychologia* **9**, 97–113. (doi:10.1016/0028-3932(71)90067-4)

713 46. Vine S, Moore L, Wilson M. 2011 Quiet eye training facilitates competitive putting performance
714 in elite golfers. *Front. Psychol.* **2**, 8. (doi:0.3389/fpsyg.2011.00008)

715 47. Cooke A, Kavussanu M, McIntyre D, Ring C. 2010 Psychological, muscular and kinematic
716 factors mediate performance under pressure. *Psychophysiology* **47**, 1109–1118.
717 (doi:10.1111/j.1469-8986.2010.01021.x)

718 48. Chhabra A, Jensen R V. 1989 Direct determination of the $f(\alpha)$ singularity spectrum. *Phys. Rev.*
719 *Lett.* **62**, 1327–1330. (doi:10.1103/PhysRevLett.62.1327)

720 49. Shannon CE. 1948 A mathematical theory of communication. *Bell Syst. Tech. J.* **27**, 379–423.
721 (doi:10.1002/j.1538-7305.1948.tb01338.x)

722 50. Schreiber T, Schmitz A. 1996 Improved surrogate data for nonlinearity tests. *Phys. Rev. Lett.* **77**,
723 635–638. (doi:10.1103/PhysRevLett.77.635)

724 51. Bates D, Sarkar D, Bates M, Matrix L. 2007 The lme4 package.

725 52. Allison PD. 1977 Testing for interaction in multiple regression. *Am. J. Sociol.* **83**, 144–153.
726 (doi:10.1086/226510)

727 53. Liphart J, Gallichio J, Tilson JK, Pei Q, Wu SS, Duncan PW. 2015 Concordance and
728 discordance between measured and perceived balance and the effect on gait speed and falls
729 following stroke. *Clin. Rehabil.* **30**, 294–302. (doi:10.1177/0269215515578294)

730 54. Williams AM. 2016 Quiet eye vs. noisy brain: The eye like the brain is always active–comment
731 on Vickers. *Curr. Issues Sport Sci.* **1**, 116. (doi:10.15203/CISS_2016.116)

55. Barlow HB. 1963 Slippage of contact lenses and other artefacts in relation to fading and regeneration of supposedly stable retinal images. *Q. J. Exp. Psychol.* **15**, 36–51. (doi:10.1080/17470216308416550)

56. Coppola D, Purves D. 1996 The extraordinarily rapid disappearance of entopic images. *Proc. Natl. Acad. Sci.* **93**, 8001–8004. (doi:10.1073/pnas.93.15.8001)

57. Ditchburn RW, Ginsborg BL. 1952 Vision with a stabilized retinal image. *Nature* **170**, 36–37. (doi:10.1038/170036a0)

58. Martinez-Conde S, Macknik SL, Troncoso XG, Dyar TA. 2006 Microsaccades counteract visual fading during fixation. *Neuron* **49**, 297–305. (doi:10.1016/j.neuron.2005.11.033)

59. Krueger E, Schneider A, Chavaillaz A, Groner R, Sawyer BD, Sonderegger A, Hancock PA. 2019 Microsaccades distinguish looking from seeing. *J. Eye Mov. Res.* **12**, 2.

60. Murnaghan CD, Carpenter MG, Chua R, Inglis JT. 2016 Keeping still doesn't "make sense": Examining a role for movement variability by stabilizing the arm during a postural control task. *J. Neurophysiol.* **117**, 846–852. (doi:10.1152/jn.01150.2015)

61. Gallicchio G, Cooke A, Ring C. 2017 Practice makes efficient: Cortical alpha oscillations are associated with improved golf putting performance. *Sport. Exerc. Perform. Psychol.* **6**, 89–102. (doi:10.1037/spy0000077)

62. Gallicchio G, Cooke A, Ring C. 2016 Lower left temporal-frontal connectivity characterizes expert and accurate performance: High-alpha T7-Fz connectivity as a marker of conscious processing during movement. *Sport. Exerc. Perform. Psychol.* **5**, 14–24. (doi:10.1037/spy0000055)

63. Vaz DV, Silva PL, Mancini MC, Carello C, Kinsella-Shaw J. 2017 Towards an ecologically grounded functional practice in rehabilitation. *Hum. Mov. Sci.* **52**, 117–132. (doi:10.1016/j.humov.2017.01.010)

64. Holt KG, Wagenaar RO, Saltzman E. 2010 A dynamic systems: Constraints approach to rehabilitation. *Brazilian J. Phys. Ther.* **14**, 446–463. (doi:10.1590/S1413-35552010000600002)

65. Harrison SJ, Stergiou N. 2015 Complex adaptive behavior and dexterous action. *Nonlinear Dynamics. Psychol. Life Sci.* **19**, 345–394.

66. Ivanov PC, Nunes Amaral LA, Goldberger AL, Havlin S, Rosenblum MG, Stanley HE, Struzik ZR. 2001 From 1/*f* noise to multifractal cascades in heartbeat dynamics. *Chaos An Interdiscip. J. Nonlinear Sci.* **11**, 641–652. (doi:10.1063/1.1395631)

67. Lipsitz LA, Goldberger AL. 1992 Loss of 'complexity' and aging: Potential applications of fractals and chaos theory to senescence. *JAMA* **267**, 1806–1809. (doi:10.1001/jama.1992.03480130122036)

766 68. Lipsitz LA. 2002 Dynamics of stability: The physiologic basis of functional health and frailty.
767 *Journals Gerontol. Ser. A* **57**, B115–B125. (doi:10.1093/gerona/57.3.B115)

768 69. Morales CJ, Kolaczyk ED. 2002 Wavelet-based multifractal analysis of human balance. *Ann.*
769 *Biomed. Eng.* **30**, 588–597. (doi:10.1114/1.1478082)

770 70. Shimizu YU, Thurner S, Ehrenberger K. 2002 Multifractal spectra as a measure of complexity in
771 human posture. *Fractals* **10**, 103–116. (doi:10.1142/S0218348X02001130)

772 71. Muñoz-Diosdado A. 2005 A non linear analysis of human gait time series based on multifractal
773 analysis and cross correlations. *J. Phys. Conf. Ser.* **23**, 87–95. (doi:10.1088/1742-6596/23/1/010)

774 72. West BJ, Scafetta N. 2003 Nonlinear dynamical model of human gait. *Phys. Rev. E* **67**, 51917.
775 (doi:10.1103/PhysRevE.67.051917)

776 73. Ashkenazy Y, M. Hausdorff J, Ch. Ivanov P, Eugene Stanley H. 2002 A stochastic model of
777 human gait dynamics. *Phys. A Stat. Mech. its Appl.* **316**, 662–670. (doi:10.1016/S0378-
778 4371(02)01453-X)

779 74. Schmitt DT, Ivanov PC. 2007 Fractal scale-invariant and nonlinear properties of cardiac
780 dynamics remain stable with advanced age: A new mechanistic picture of cardiac control in
781 healthy elderly. *Am. J. Physiol. Integr. Comp. Physiol.* **293**, R1923–R1937.
782 (doi:10.1152/ajpregu.00372.2007)

783 75. Friston K, Breakspear M, Deco G. 2012 Perception and self-organized instability. *Front.*
784 *Comput. Neurosci.* **6**, 44. (doi:10.3389/fncom.2012.00044)

785 76. Oftadeh R, Haghpanah B, Vella D, Boudaoud A, Vaziri A. 2014 Optimal fractal-like
786 hierarchical honeycombs. *Phys. Rev. Lett.* **113**, 104301. (doi:10.1103/PhysRevLett.113.104301)

787 77. Schlesinger MF, Klafter J. 1986 Lévy walks versus Lévy flights. In *Growth and Form* (eds HE
788 Stanley, N Ostrowski), pp. 279–283. Amsterdam, Netherlands: Martinus Nijhoff.

789 78. Reynolds AM. 2015 Liberating Lévy walk research from the shackles of optimal foraging. *Phys.*
790 *Life Rev.* **14**, 59–83. (doi:10.1016/j.plrev.2015.03.002)

791 79. Dixon JA, Holden JG, Mirman D, Stephen DG. 2012 Multifractal dynamics in the emergence of
792 cognitive structure. *Top. Cogn. Sci.* **4**, 51–62. (doi:10.1111/j.1756-8765.2011.01162.x)

793 80. Diniz A *et al.* 2011 Contemporary theories of 1/*f* noise in motor control. *Hum. Mov. Sci.* **30**,
794 889–905. (doi:10.1016/j.humov.2010.07.006)

795 81. Kello CT. 2018 Editor's introduction and review: Coordination and context in cognitive science.
796 *Top. Cogn. Sci.* **10**, 6–17. (doi:10.1111/tops.12302)

797 82. Wagenmakers E-J, van der Maas HLJ, Farrell S. 2012 Abstract concepts require concrete
798 models: Why cognitive scientists have not yet embraced nonlinearly coupled, dynamical, self-
799 organized critical, synergistic, scale-free, exquisitely context-sensitive, interaction-dominant,

multifractal, interdependent b. *Top. Cogn. Sci.* **4**, 87–93. (doi:10.1111/j.1756-8765.2011.01164.x)

83. Kelty-Stephen DG, Stirling LA, Lipsitz LA. 2016 Multifractal temporal correlations in circle-tracing behaviors are associated with the executive function of rule-switching assessed by the Trail Making Test. *Psychol. Assess.* **28**, 171–180. (doi:10.1037/pas0000177)

84. Meyer M, Stiedl O, Kerman B. 2003 Discrimination by multifractal spectrum estimation of human heartbeat interval dynamics. *Fractals* **11**, 195–204. (doi:10.1142/S0218348X03002063)

85. Haken H, Kelso JAS, Bunz H. 1985 A theoretical model of phase transitions in human hand movements. *Biol. Cybern.* **51**, 347–356. (doi:10.1007/BF00336922)

86. Park H, Turvey MT. 2008 Imperfect symmetry and the elementary coordination law. In *Coordination: Neural, Behavioral and Social Dynamics* (eds A Fuchs, VK Jirsa), pp. 3–25. Berlin, Heidelberg: Springer Berlin Heidelberg. (doi:10.1007/978-3-540-74479-5_1)

87. Stoffregen TA, Mantel B, Bardy BG. 2017 The senses considered as one perceptual system. *Ecol. Psychol.* **29**, 165–197. (doi:10.1080/10407413.2017.1331116)

88. Wallot S, O'Brien B, Coey CA, Kelty-Stephen D. 2015 Power-law fluctuations in eye movements predict text comprehension during connected text reading. In *Proceedings of the 37th Annual Meeting of the Cognitive Science Society* (eds DC Noelle, R Dale, AS Warlaumont, J Yoshimi, T Matlock, CD Jennings), pp. 2583–2588.

89. Mangalam M, Carver NS, Kelty-Stephen DG. 2020 Global broadcasting of local fractal fluctuations in a bodywide distributed system supports perception via effortful touch. *Chaos, Solitons & Fractals* **135**, 109740. (doi:10.1016/j.chaos.2020.109740)

90. Mangalam M, Carver NS, Kelty-Stephen DG. 2020 Multifractal signatures of perceptual processing on anatomical sleeves of the human body. *J. R. Soc. Interface* **17**, 20200328. (doi:10.1098/rsif.2020.0328)

91. Kelty-Stephen DG, Dixon JA. 2014 Interwoven fluctuations during intermodal perception: Fractality in head sway supports the use of visual feedback in haptic perceptual judgments by manual wielding. *J. Exp. Psychol. Hum. Percept. Perform.* **40**, 2289–2309. (doi:10.1037/a0038159)

92. Stephen D, Anastas J, Dixon J. 2012 Scaling in cognitive performance reflects multiplicative multifractal cascade dynamics. *Front. Physiol.* **3**, 102. (doi:10.3389/fphys.2012.00102)

93. Anastas JR, Kelty-Stephen DG, Dixon JA. 2014 Executive function as an interaction-dominant process. *Ecol. Psychol.* **26**, 262–282. (doi:10.1080/10407413.2014.957985)

94. Kardan O, Adam KCS, Mance I, Churchill NW, Vogel EK, Berman MG. 2020 Distinguishing cognitive effort and working memory load using scale-invariance and alpha suppression in EEG. *Neuroimage* **211**, 116622. (doi:10.1016/j.neuroimage.2020.116622)

95. Kardan O, Layden E, Choe KW, Lyu M, Zhang X, Beilock SL, Rosenberg MD, Berman MG. 2020 Scale-invariance in brain activity predicts practice effects in cognitive performance. *bioRxiv* , 114959. (doi:10.1101/2020.05.25.114959)

96. Kelty-Stephen DG, Mirman D. 2013 Gaze fluctuations are not additively decomposable: Reply to Bogartz and Staub. *Cognition* **126**, 128–134. (doi:10.1016/j.cognition.2012.09.002)

97. Ingber DE. 2006 Cellular mechanotransduction: Putting all the pieces together again. *FASEB J.* **20**, 811–827. (doi:10.1096/fj.05-5424rev)

98. Turvey MT, Fonseca ST. 2014 The medium of haptic perception: A tensegrity hypothesis. *J. Mot. Behav.* **46**, 143–187. (doi:10.1080/00222895.2013.798252)

99. Schleip R, Mechsner F, Zorn A, Klingler W. 2014 The bodywide fascial network as a sensory organ for haptic perception. *J. Mot. Behav.* **46**, 191–193. (doi:10.1080/00222895.2014.880306)

100. Moore LJ, Vine SJ, Freeman P, Wilson MR. 2013 Quiet eye training promotes challenge appraisals and aids performance under elevated anxiety. *Int. J. Sport Exerc. Psychol.* **11**, 169–183. (doi:10.1080/1612197X.2013.773688)

849 **Table 1.** Training instructions given to the quiet-eye and technical groups during the training phase.

quiet-eye (QE) training instructions	**technical training instructions**
assume your stance, and ensure your gaze is located on the back of the ball	take your stance with your legs shoulder-width apart
after setting up over the ball, fix your gaze on the hole	set your position so that your head is directly above the ball looking down
make no more than three fixations towards the hole	keep your clubhead square to the ball
your final fixation should be a quiet eye on the back of the ball. The onset of the quiet eye should occur before the stroke begins and last for 2 to 3s	allow your arms and shoulders to remain loose
ensure you direct gaze towards the clubhead during the putting stroke	the putting action should be pendulum-like, making sure that you accelerate through the ball
the quiet eye should remain on the green for 200 to 300ms after the club contacts the ball	after contact, follow through but keep your head still and facing down

850 Source: Adapted from [100].

851 **Table 2.** Logistic regression modeling of successful shots.

predictor	***b***	***s.e.m.***	***p*** *
intercept	–2.85	0.48	**< 0.0001**
QE	0.20	0.30	0.51
perturbation	–0.22	0.43	0.60
QE × perturbation	–1.16	0.65	0.07
block	0.24	0.13	**0.06**
RMS_{Acc}	4.05	1.34	**< 0.01**
W_{MF}	–7.25	2.94	**< 0.05**

852 *boldfaced values indicate statistical significance at the alpha level of 0.05.

853 **Table 3.** Subset of Poisson regression model including main and interaction effects non-multifractal
854 and multifractal measures of sway, perturbation of eye height, and time

predictor	*b*	*s.e.m.*	*p**
effects of non-multifractal measures of sway (see Section 3.2.1.)			
MSD_{acc}	-8.80×10^{0}	1.67×10^{-1}	**< 0.0001**
$Mean_{disp}$	-2.91×10^{2}	1.33×10^{1}	**< 0.0001**
SD_{disp}	4.43×10^{0}	1.64×10^{0}	**< 0.01**
$MSD_{acc} \times Mean_{disp}$	1.97×10^{4}	1.00×10^{1}	**< 0.0001**
$MSD_{acc} \times SD_{disp}$	-3.11×10^{3}	1.03×10^{1}	**< 0.0001**
$Mean_{disp} \times SD_{disp}$	2.56×10^{4}	1.05×10^{1}	**< 0.0001**
$MSD_{acc} \times Mean_{disp} \times SD_{disp}$	-1.04×10^{5}	1.08×10^{1}	**< 0.0001**
effects of multifractal measures of sway and interactions with time (see Section 3.2.2.)			
W_{MF}	1.80×10^{0}	1.29×10^{-1}	**< 0.0001**
t_{MF}	2.21×10^{-4}	1.05×10^{-3}	0.83
$W_{MF} \times t_{MF}$	-5.93×10^{-3}	8.27×10^{-3}	0.48
$t_{MF} \times trial_{block}$(Linear)	1.36×10^{-2}	9.82×10^{-3}	0.17
$t_{MF} \times trial_{block}$(Quadratic)	-8.93×10^{-2}	1.15×10^{-2}	**< 0.0001**
$t_{MF} \times trial_{block}$(Cubic)	-1.08×10^{-2}	1.14×10^{-2}	0.34
interactions of multifractal measures of sway with perturbation (see Section 3.2.3.)			
QE × W_{MF}	-1.04×10^{-0}	2.03×10^{-1}	**< 0.0001**
QE × t_{MF}	-1.85×10^{-3}	1.30×10^{-3}	0.16
QE × $W_{MF} \times t_{MF}$	-4.59×10^{-3}	1.09×10^{-2}	0.67
perturbation × W_{MF}	-1.50×10^{0}	3.12×10^{-1}	**< 0.0001**
perturbation × t_{MF}	4.57×10^{-3}	2.85×10^{-3}	0.11
perturbation × $W_{MF} \times t_{MF}$	1.54×10^{-1}	3.15×10^{-2}	**< 0.0001**
QE × perturbation × W_{MF}	2.12×10^{0}	4.91×10^{-1}	**< 0.0001**
QE × perturbation × t_{MF}	8.62×10^{-3}	4.18×10^{-3}	**< 0.05**
QE × perturbation × $W_{MF} \times t_{MF}$	-2.21×10^{-1}	4.97×10^{-2}	**< 0.0001**
interactions of multifractal measures with perturbation and time (see Section 3.2.4.)			
QE × $trial_{block}$(Linear) × t_{MF}	-3.73×10^{-2}	1.46×10^{-2}	**< 0.05**
QE × $trial_{block}$(Quadratic) × t_{MF}	-1.85×10^{-1}	1.66×10^{-2}	**< 0.0001**
QE × $trial_{block}$(Cubic) × t_{MF}	1.13×10^{-1}	1.73×10^{-2}	**< 0.0001**
perturbation × $trial_{block}$(Linear) × t_{MF}	3.83×10^{-1}	5.28×10^{-2}	**< 0.0001**
perturbation × $trial_{block}$(Quadratic) × t_{MF}	4.07×10^{-1}	5.20×10^{-2}	**< 0.0001**
perturbation × $trial_{block}$(Cubic) × t_{MF}	5.39×10^{-1}	4.45×10^{-2}	**< 0.0001**
QE × perturbation × $trial_{block}$(Linear) × t_{MF}	-2.71×10^{-1}	6.11×10^{-2}	**< 0.0001**
QE × perturbation × $trial_{block}$(Quadratic) × t_{MF}	5.24×10^{-1}	6.14×10^{-2}	**< 0.0001**
QE × perturbation × $trial_{block}$(Cubic) × t_{MF}	-7.90×10^{-1}	5.79×10^{-2}	**< 0.0001**

855 *boldfaced values indicate statistical significance at the alpha level of 0.05.

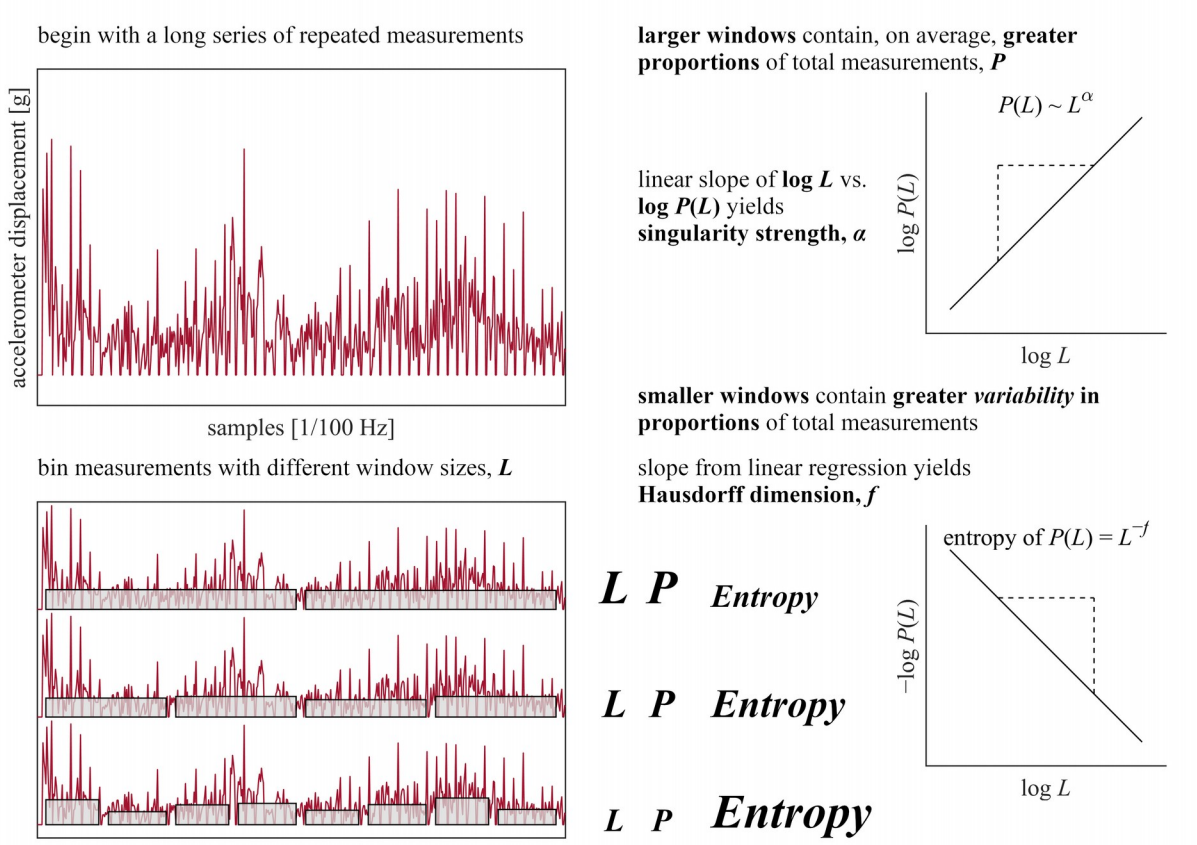

Figure 1. Schematic of Chhabra and Jensen's [48] method used to estimate multifractal spectrum $f(\alpha)$ (Part-1). See Section 2.4.1. for further details.

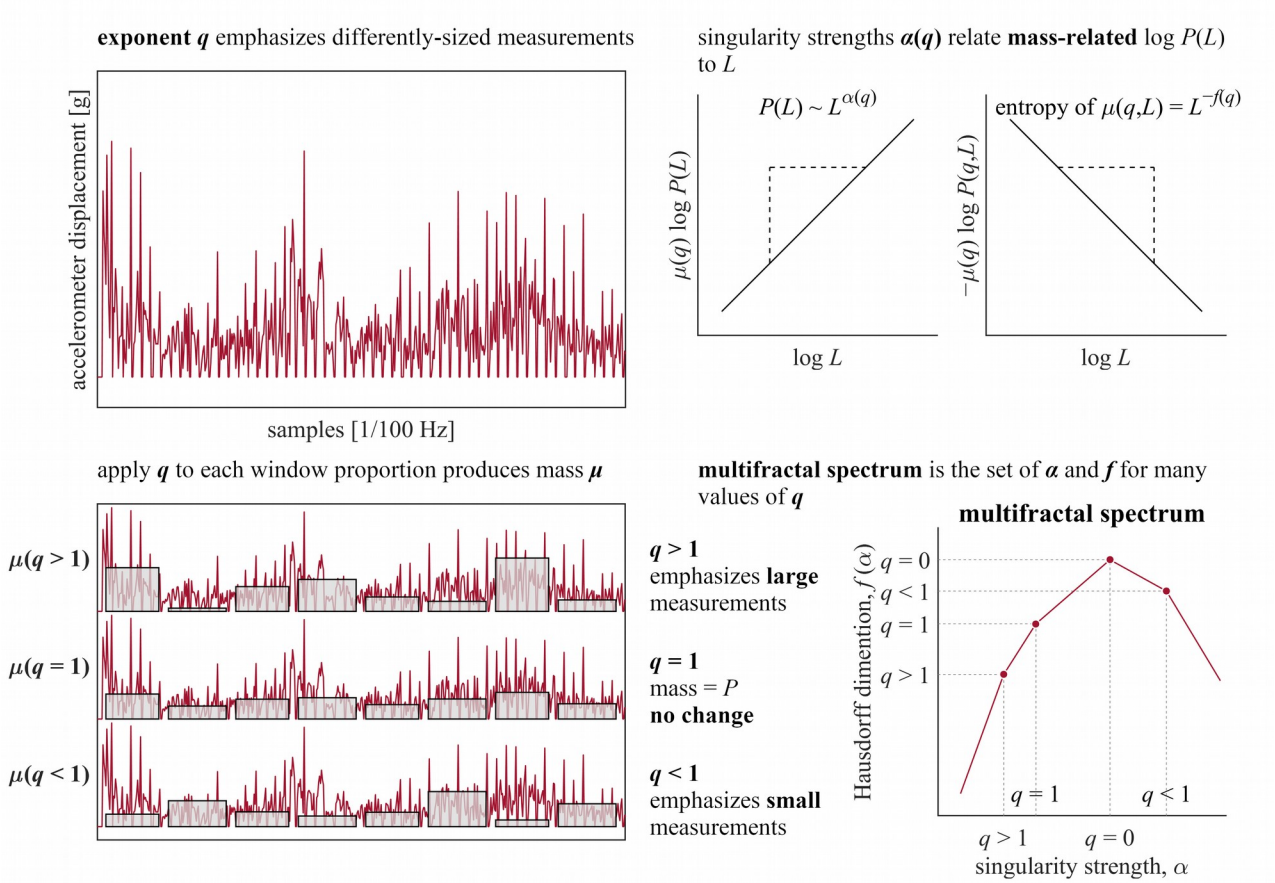

Figure 2. Schematic of Chhabra and Jensen's [48] method used to estimate multifractal spectrum $f(\alpha)$ (Part-2). See Section 2.4.1. for further details.

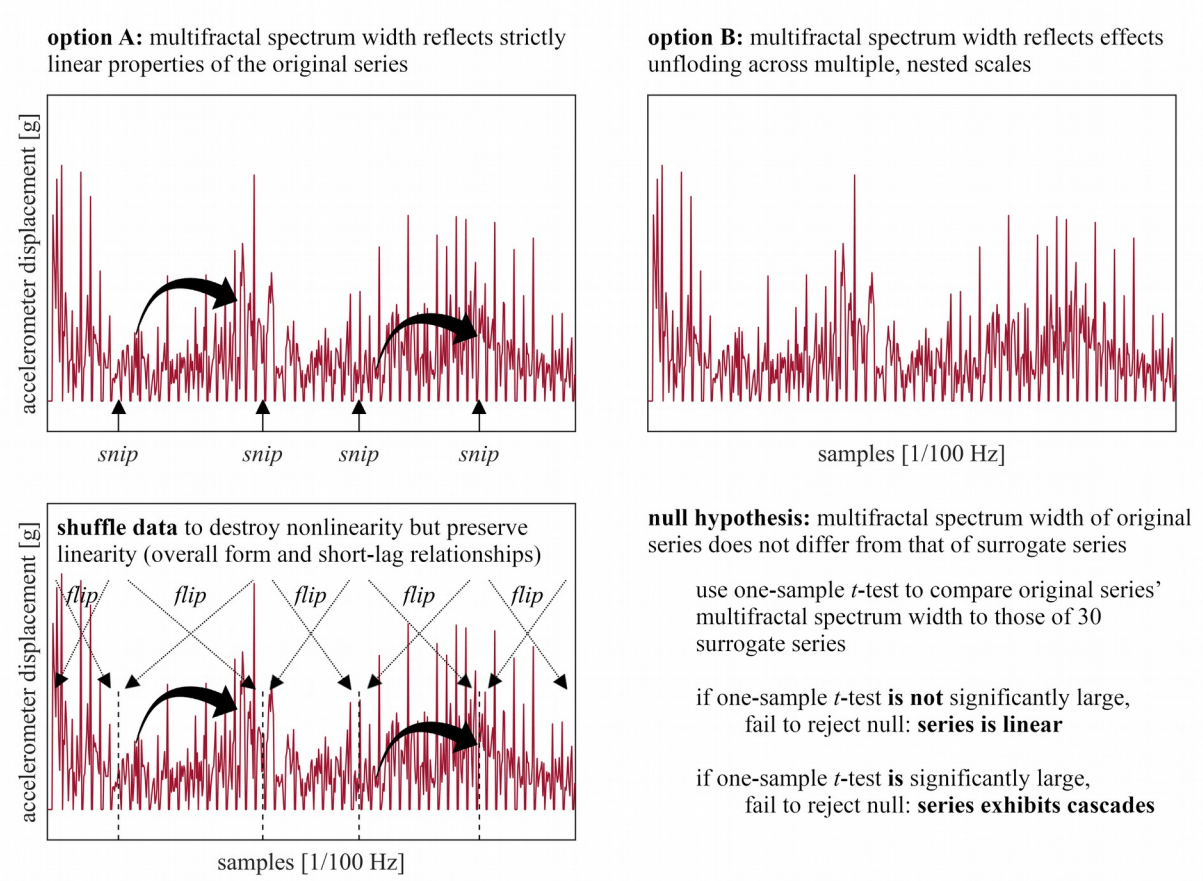

Figure 3. Surrogate analysis used to identify whether a series exhibits multifractality due to nonlinearity (cascades). See Section 2.4.2. for further details.

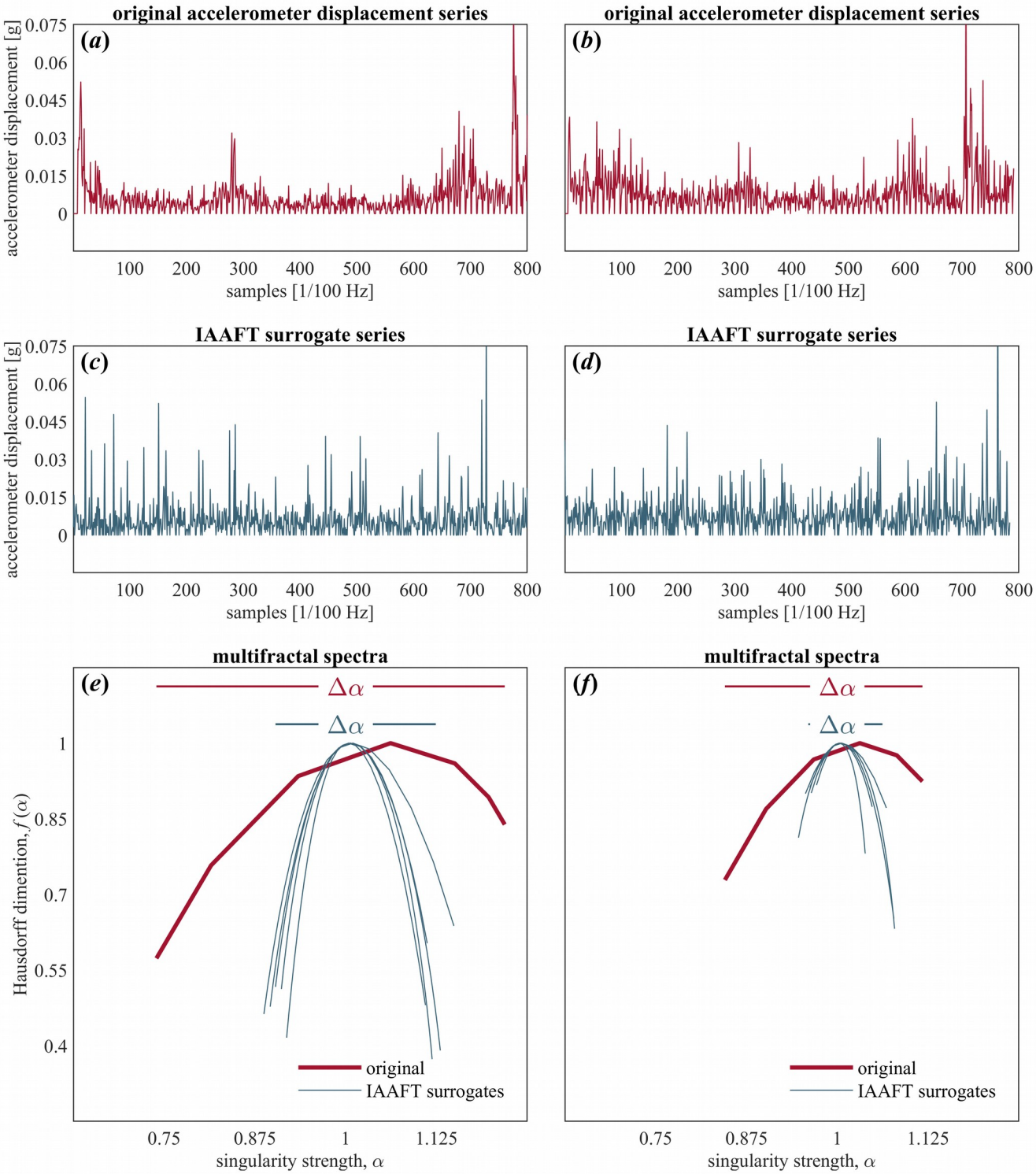

Figure 4. Multifractal analysis. (*a*, *b*) Representative original accelerometer displacement series. (*c*, *d*) Representative IAAFT surrogate series of the original accelerometer displacement series in *a* and *b*. (*e*, *f*) Multifractal spectrum ($f(\alpha)$, α) of original series in *a* and *b*, and those of their five representative IAAFT surrogates.

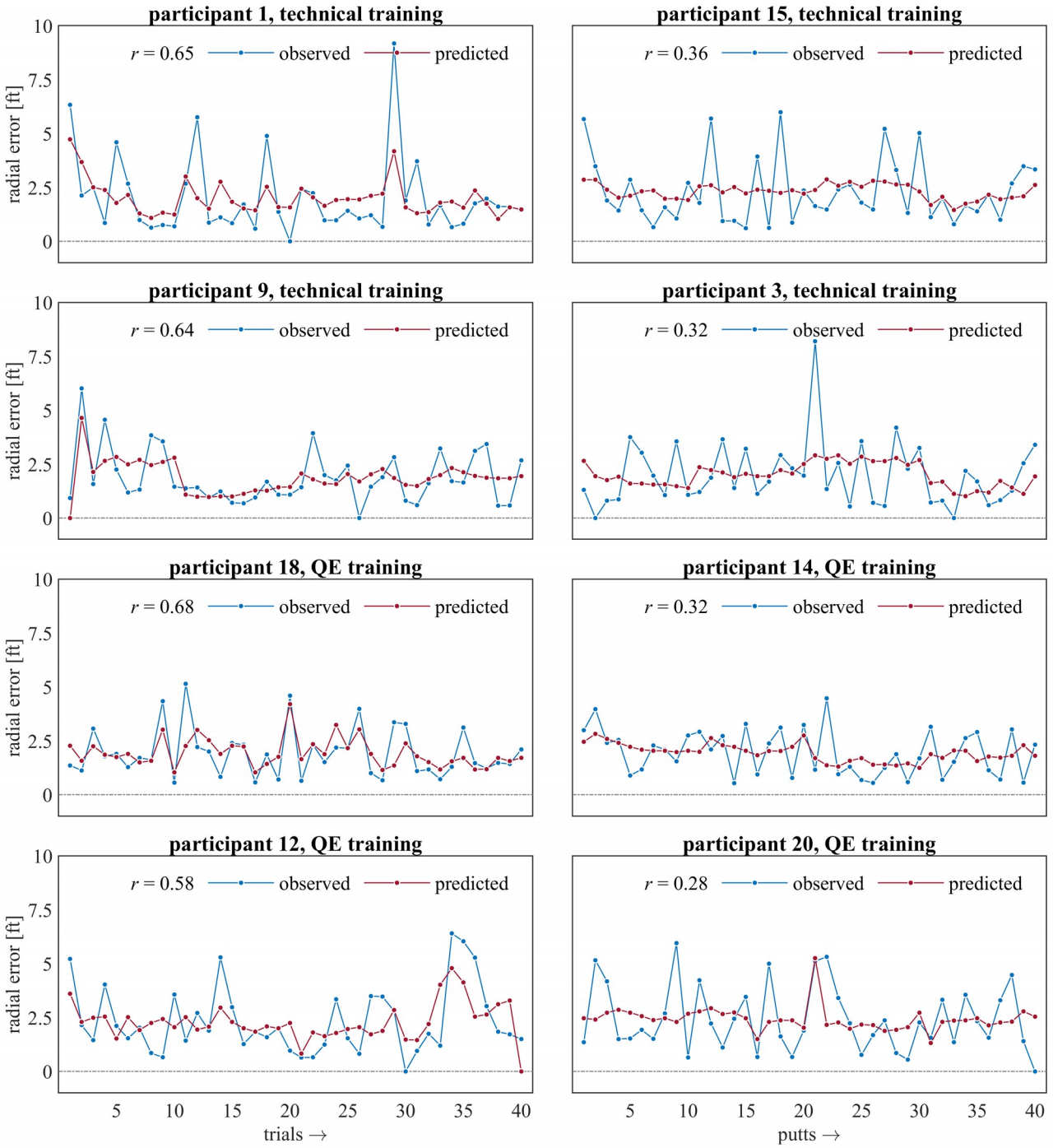

Figure 5. The observed trial-by-trial radial error and trial-by-trial model predictions on the same axis for four participants each from the technical (top four panels) and QE-trained (bottom four panels) groups, respectively. The representation includes two participants each with the highest (left panels) and lowest (right panels) Pearson's correlation coefficient r indicating the strength of relationship between the observed and predicted radial errors.

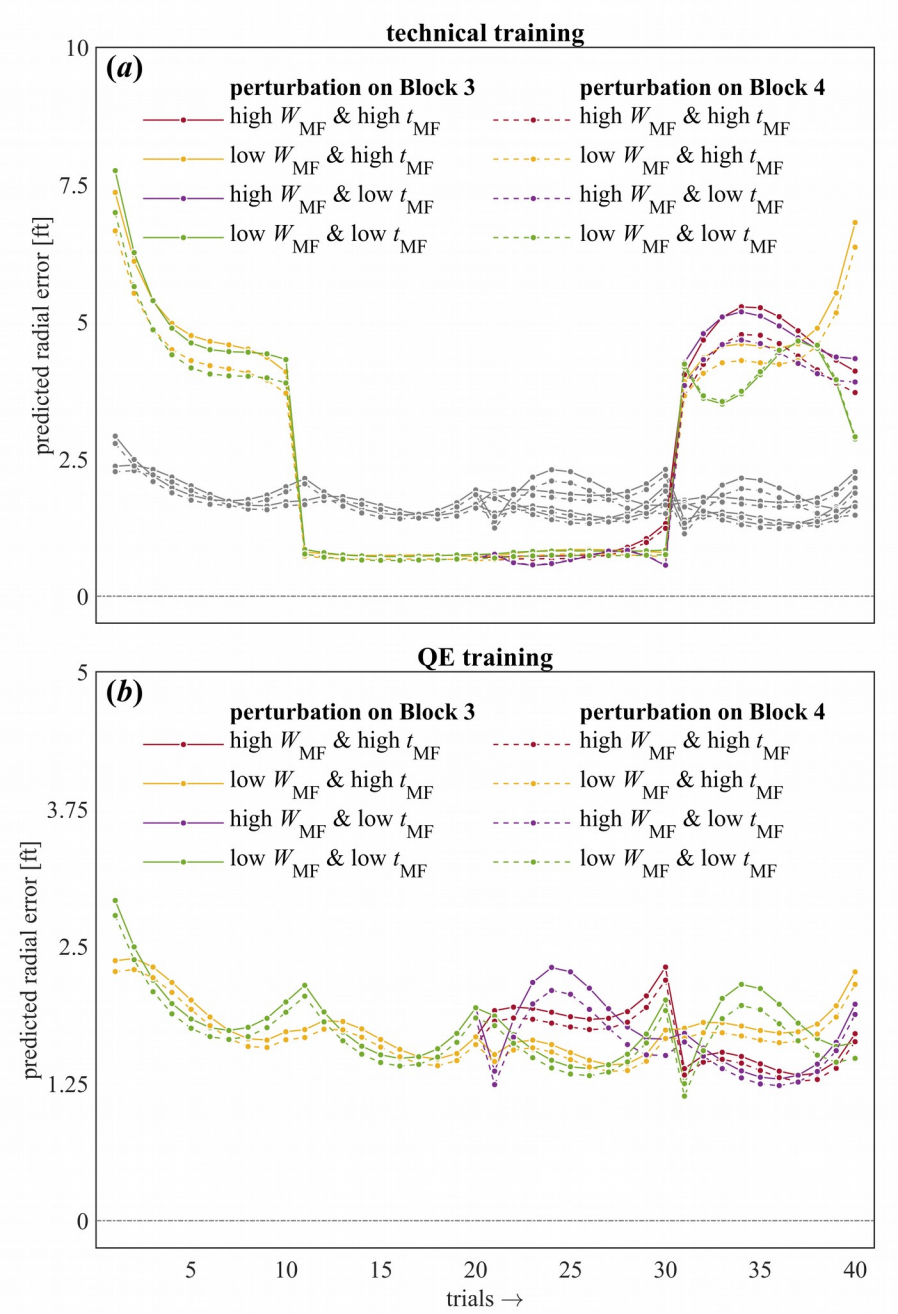

871 **Figure 6.** Trial-by-trial model predictions of radial error for the two participant groups. (*a*) Technical-
872 trained group. (*b*) QE-trained group.

873 **Supplementary Table S1.** Subset of Poisson regression model output including main and interaction
874 effects of time and perturbation of eye height.

predictor	***b***	***s.e.m.***	***p*** *
intercept	9.04×10^{0}	3.29×10^{-1}	**< 0.0001**
$trial_{exp}$(Linear)	4.70×10^{1}	2.26×10^{0}	**< 0.0001**
$trial_{exp}$(Quadratic)	3.08×10^{1}	1.20×10^{0}	**< 0.0001**
$trial_{exp}$(Cubic)	-1.78×10^{0}	1.54×10^{-1}	**< 0.0001**
$trial_{block}$(Linear)	2.17×10^{1}	9.34×10^{-1}	**< 0.0001**
$trial_{block}$(Quadratic)	9.60×10^{-1}	2.63×10^{-1}	**< 0.001**
$trial_{block}$(Cubic)	-1.62×10^{0}	2.57×10^{-1}	**< 0.0001**
block	-1.41×10^{0}	1.34×10^{-1}	**< 0.0001**
block × $trial_{block}$(Linear)	-1.36×10^{1}	5.83×10^{-1}	**< 0.0001**
block × $trial_{block}$(Quadratic)	-1.10×10^{0}	1.10×10^{-1}	**< 0.001**
block × $trial_{block}$(Cubic)	6.40×10^{-1}	1.08×10^{-1}	**< 0.0001**
QE	-4.40×10^{0}	4.81×10^{-1}	**< 0.0001**
QE × $trial_{exp}$(Linear)	-6.07×10^{1}	3.54×10^{0}	**< 0.0001**
QE × $trial_{exp}$(Quadratic)	-3.21×10^{1}	1.86×10^{0}	**< 0.0001**
QE × $trial_{exp}$(Cubic)	1.03×10^{0}	2.18×10^{-1}	**< 0.0001**
QE × $trial_{block}$(Linear)	-2.41×10^{1}	1.41×10^{0}	**< 0.0001**
QE × $trial_{block}$(Quadratic)	9.35×10^{-1}	3.79×10^{-1}	**< 0.05**
QE × $trial_{block}$(Cubic)	2.24×10^{0}	3.54×10^{-1}	**< 0.0001**
QE × block	1.72×10^{0}	1.96×10^{-1}	**< 0.0001**
QE × block × $trial_{block}$(Linear)	1.56×10^{1}	8.99×10^{-1}	**< 0.0001**
QE × block × $trial_{block}$(Quadratic)	1.31×10^{0}	1.63×10^{-1}	**< 0.0001**
QE × block × $trial_{block}$(Cubic)	-5.57×10^{-1}	1.54×10^{-1}	**< 0.01**
Perturbation	3.90×10^{-2}	3.01×10^{-1}	0.90
QE × perturbation	8.73×10^{-2}	4.26×10^{-1}	0.84
perturbation × $trial_{block}$(Linear)	1.58×10^{0}	3.02×10^{-1}	**< 0.0001**
perturbation × $trial_{block}$(Quadratic)	1.25×10^{0}	3.08×10^{-1}	**< 0.001**
perturbation × $trial_{block}$(Cubic)	-2.42×10^{0}	2.97×10^{-1}	**< 0.0001**
QE × perturbation × $trial_{block}$(Linear)	-1.16×10^{0}	4.44×10^{-1}	**< 0.01**
QE × perturbation × $trial_{block}$(Quadratic)	-5.71×10^{0}	4.43×10^{-1}	**< 0.0001**
QE × perturbation × $trial_{block}$(Cubic)	3.39×10^{0}	4.31×10^{-1}	**< 0.0001**

875 *boldfaced values indicate statistical significance at the alpha level of 0.05.